

DOI: <http://doi.org/10.52716/jprs.v13i3.616>

## Effect of Calcination Temperature on Prepared $\gamma$ -Al<sub>2</sub>O<sub>3</sub> as Support Catalyst

Helal A. Saleem<sup>1</sup>, Ban A. Al-Tabbakh<sup>2\*</sup>, Aysar T. Jarullah<sup>1</sup><sup>1</sup>Tikrit University<sup>2</sup>Petroleum Research & Development center<sup>2\*</sup>Corresponding Author E-mail: [dr.banaltabbakh@gmail.com](mailto:dr.banaltabbakh@gmail.com)

Received 23/10/2022, Revised 28/12/2022, Accepted 11/01/2023, Published 10/09/2023

This work is licensed under a [Creative Commons Attribution 4.0 International License](https://creativecommons.org/licenses/by/4.0/).

### **Abstract**

The effect of calcination temperature on the surface properties of gamma alumina was investigated in this study, which is used as a support for multiple metal-loaded catalysts. The Sol-gel technique was used to create  $\gamma$ -Al<sub>2</sub>O<sub>3</sub> support from aluminum nitrate as a precursor at various calcination temperatures (500, 550, 600, and 650°C). Then, for each sample, characterization tests such as X-Ray fluorescence (XRF), X-Ray diffraction (XRD), Thermal gravimetric analysis (TGA), and surface area (BET) are performed to determine the optimal calcination temperature to produce highly active composite catalyst support. It has been discovered that samples calcined at 600 and 650°C have very similar properties in terms of mechanical strength, thermal stability, crystallinity, high purity, and surface properties or morphology. However, the surface area and pore volume of 600°C are thought to be superior to those of 650°C.

**Keywords:** Alumina Composite catalyst, Precipitation, Calcination temperature.

### **1. Introduction:**

Significant demand for metal oxide nanomaterials, particularly alumina (Al<sub>2</sub>O<sub>3</sub>), has piqued the interest of researchers. The synthesis of these materials is efficient, inexpensive, and environmentally friendly. There are eight different phases for alumina, including (cubic spinel), (tetragonal or orthorhombic), (cubic spinel), (monoclinic), (orthorhombic), (hexagonal), and. However, the thermally stable phase is  $\gamma$ -Al<sub>2</sub>O<sub>3</sub>. The method of synthesis influences the properties of the alumina obtained, such as purity, particle size, and chemical homogeneity.

Alumina phase transformations involve numerous crystal structures and various combinations of hydroxides and oxyhydroxides. Al<sub>2</sub>O<sub>3</sub> is well known for its high catalytic activity and has great potential as a support material for catalysis and artificial photosynthesis. [1],[2]

Because of its high surface area, porosity, and mechanical properties, alumina has many potential applications in industries and high-tech sectors. Numerous methods for the synthesis of alumina that was cost-effective and required high temperatures and pressures, such as the Bayer process, sol-gel method, control precipitation method from aluminum salts, and extraction of alumina from kaoline, had been tried. [3]

Temperature, pressure, reaction time, pyrolysis methods, type of preparation technique, and materials used in the preparation can all be changed to change the morphology of gamma alumina.

Because of its high thermal stability, gamma alumina is used as catalyst support in its synthesis, and its ability to form into small parts (spherical or cylindrical) As a result of its mechanical stability, gamma alumina is used as catalytic support in a variety of chemical reactions. Gamma Activation

Alumina is commonly used as a catalyst, auxiliary catalyst, support, and adsorption material. The method and techniques used to prepare alumina, as well as the calcination temperature, have a significant impact on its surface area and histological composition, which controls the extent of alumina gamma activity.[4]

Many studies have already been conducted on alumina nanoparticles produced using various solution-based techniques such as sol-gel hydrothermal, microwave, and microemulsions.

Ivas et.al. used a solvent-free method based on aluminum nitrate and ammonium hydrogen carbonate precursors to create  $Al_2O_3$  nanoparticles. The surface area obtained from 245 to 337  $m^2/g$  with the best crystalline size of 1.51nm.[1]

A simple method for converting waste aluminum cans into a valuable nanoparticle gamma alumina catalyst with high industrial application potential. Despite the increased crystallinity obtained at higher temperatures, investigations revealed that calcination at 550°C is convenient for producing high crystalline structures due to the energy-saving aspect. Furthermore, the pH of precipitating aluminum oxide in the neutral region is an important factor, producing a high surface area of crystalline of 311 $m^2/g$  and a nano-size product of 68.56n.[5]

Nayar. et.al. prepared  $Al_2O_3$  nanoparticles using the Chemical Precipitation (CP) and Sol-Gel Auto Combustion (SGAC) methods, and the structural behavior of the nanoparticles was compared.

At an annealing temperature of 1100 °C, nanoparticles prepared by CP gradually transformed to the thermodynamically stable  $\alpha$ -phase of alumina, whereas pure  $\alpha$ -alumina was obtained directly for nanoparticles prepared by the sol-gel method during the combustion stage. After calcining at a higher temperature, the surface morphology revealed particle agglomeration.[6]

The goal of this study is to improve the properties of prepared gamma alumina, such as surface area, pore volume, pore size, and purity by precipitation method and focusing on the effect of calcination temperature on the final phase where the samples were calcined at different temperatures (500, 550, 600, and 650 °C).

## 2. Experimental work

### 2.1 Materials and preparation method

The precipitation and sol-gel technique is used to prepare  $\gamma$ -alumina and the chemicals and materials utilized are mentioned in Table (1).

**Table (1) properties of materials**

<i>Chemicals and Materials</i>	<i>Purity%</i>	<i>Company</i>
<i>Aluminum Nitrate <math>Al(NO_3)_3 \cdot 9H_2O</math></i>	<i>97</i>	<i>GCC</i>
<i>Ammonium hydroxide <math>(NH_4OH)</math></i>	<i>25</i>	<i>GCC</i>
<i>Ethanol <math>(C_2H_5OH)</math></i>	<i>100</i>	<i>Hayaman</i>
<i>Ammonia Molybdate <math>(NH_4)_6Mo_3O_7 \cdot 4H_2O</math></i>	<i>98</i>	<i>BDH Limited</i>
<i>Ferric nitrate hydrate <math>Fe(NO_3)_3 \cdot 9H_2O</math></i>	<i>98</i>	<i>Himedia</i>

### 2.2 preparation of nano $\gamma$ -alumina

More efficient catalyst supports (nano-alumina) can be prepared and doped. The catalyst will then be characterized using advanced surface techniques such as Brunauer-Emmett Teller (BET), X-ray diffraction (XRD), scanning electron microscopy (SEM), thermogravimetric analyses (TGA), Crush Strength of Extruded Catalyst (crash test), and infrared spectroscopy (FT-IR).

The preparation process of  $\gamma$ -alumina is carried out by the precipitation method and can be summarized by the following steps:

150 g of  $\text{Al}(\text{NO}_3)_3 \cdot 9\text{H}_2\text{O}$  is dissolved in 180 mL of deionized water. Under constant magnetic stirring, drops of ammonium hydroxide are slowly added until the solution mixture is turned into a foaming solution as shown in Figure (1). The pH of the solution mixture is initially recorded at 2.4, then gradually increased sharply from 2.4 to 7.8 during preparing alumina.[7],[8]



**Fig. (1): Addition of ammonium hydroxide to aluminum nitrate**

The foaming solution was then treated with 50 ml of water and 50 ml of ethanol to eliminate any insoluble contaminants. As shown in Figure (2), the sol-gel is subsequently filtered using a vacuum filter pump and filter paper.

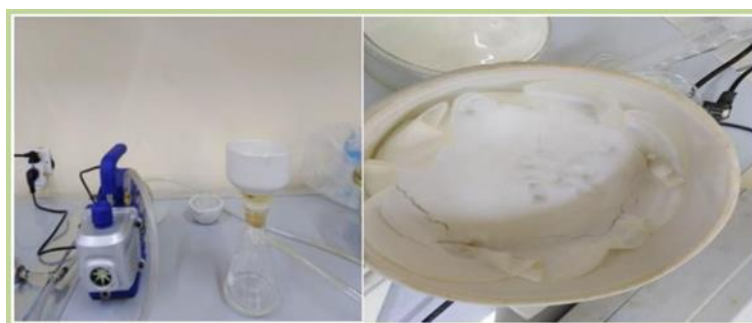


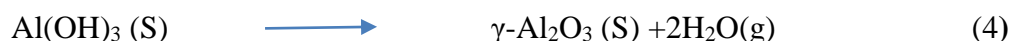
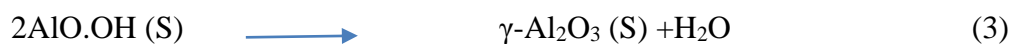
**Fig. (2): Drying and filtration stage by a vacuum pump**

The filtered foaming solution was dried for 12 hours in a drying furnace set at  $120^\circ\text{C}$ . The drying process causes the solution gel to solidify until the volume of the foaming solution shrinks and the color changes from grey to white. The dried sample was subsequently crushed using mortar to remove the particle aggregation, as illustrated in Figure (3).



**Fig. (3): Prepared gamma alumina after drying.**

After that, the samples were calcined at different values of temperature at 500, 550, 600, and 650°C for 6 hr by using a furnace to obtain the Nano  $\gamma$ - alumina according to the following equations 1-4:



The procedure of calcination was carried out in steps where the temperature is increased at a rate of 10 °C/min to 250°C for 1h then to 450 °C for 1 hr and finally to 500, 550, 600, and 650°C for 4 h. The powder was cooled down to room temperature then the powder was crashed by a grinder machine to obtain the final result of the nano $\gamma$ -alumina as shown in Figure (4).[3]



**Fig. (4): Final prepared Nano  $\gamma$ -alumina**

### **3. Characterizations of catalysts.**

#### **3.1 X-ray diffraction (XRD)**

The prepared  $\gamma\text{-Al}_2\text{O}_3$  catalyst support powder will be tested for crystallinity using XRD employing a CuK, Nickel filter with wavelength ( $= 1.5406 \text{ \AA}$ ) and the results are recorded for

2 thetas ranging from 10.000 to 80.000 degrees at a scanning speed of 5 degrees/min. The Sharif University of Technology conducts the tests.

### **3.2 X-ray fluorescence (XRF)**

The chemical compositions of the prepared catalyst samples are measured using X-Ray Fluorescence type Spectro xerox, Ametek (Germany). The analysis is carried out in the Geology Department / College of Science / Baghdad University by pressing 4 grams of sample in a disk form and passing Helium through it.

### **3.3 Brunauer, Emmett, and Teller (BET) method**

Surface area, nitrogen Adsorption–Desorption Isotherms, and pore volume measurement of the prepared samples are performed using Brunauer, Emmett, and Teller (BET) method by Thermo Analyzer (USA) with degassing step by using nitrogen under vacuum condition at 250 °C and 6 hr. The tests are performed at the laboratory of the Petroleum Research and Development Center (PRDC)/ Ministry of Oil / Iraq.

### **3.4 Fourier transform infrared (FTIR)**

FTIR test is performed at PRDC Laboratory to investigate the acid sites of the prepared sample of  $\gamma$ -Al<sub>2</sub>O<sub>3</sub>.

### **3.5 Thermal gravimetric analysis (TGA)**

The TGA is carried out at the Petroleum Research and Development Center (PRDC) laboratory to examine sample mass loss as temperature rises.

## **4. Results and Discussion**

characterization of the produced - alumina and composite catalysts by X-Ray Diffraction (XRD), X-Ray Fluorescence (XRF), Thermal gravimetric analysis (TGA), surface area (BET), Fourier Transform Infrared (FTIR), and Particle Distribution are presented and discussed. The effect of process parameters (temperature of the reaction, batch time, and type of catalyst) on the sulfur conversion will also be discussed in this chapter.

### **4.1 XRF of the prepared gamma-alumina**

X-ray fluorescence is used to assess the elemental composition of produced gamma-alumina (XRF). The greatest purity of the produced -alumina, as indicated in Table (2), is achieved for the sample that was calcined at 650 °C, which is equivalent to 97.786 percent.

Table (2) XRF of the prepared  $\gamma$ -alumina at different temperatures

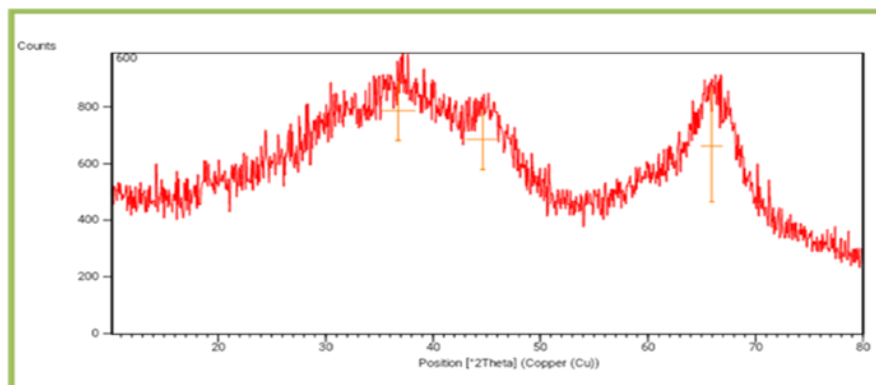
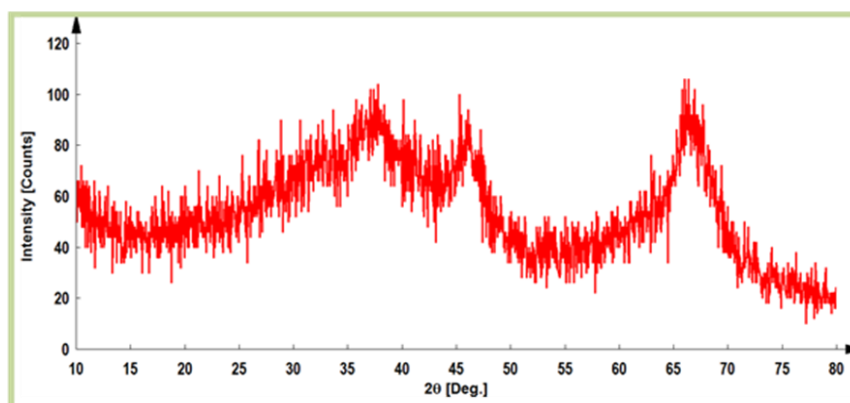
Compound Name	$\gamma$ -alumina calcined. (500 °C)	$\gamma$ -alumina calcined. (550 °C)	$\gamma$ -alumina calcined. (600° C)	$\gamma$ -alumina calcined. (650 °C)
$Al_2O_3$	94.844	97.156	97.379	97.786
$SiO_2$	4.0166	1.5779	1.327	1.312
$SO_3$	1.1392	1.0499	1.1487	1.1433
$CaO$	-----	0.21659	0.13958	0.12458

Table (2) shows that raising the calcination temperature leads to an improvement in alumina purity, which may be ascribed to a decrease in the proportion of impurity oxides vented as well as an increase in alumina crystallization.

#### 4.2 Gamma-alumina X-ray diffraction (XRD)

The use of X-ray diffraction (XRD) to characterize crystalline materials is a non-destructive technology. Provided are crystal structure, phase, preferred crystal orientation (texture), and other structural parameters such as average grain size and crystallization. The average crystallite or grain size of catalysts may be estimated using XRD [9]. The intensity of the peaks with 2 of the prepared gamma-alumina calcined at different temperatures (500, 550, 600, and 650°C) differs from one another, as shown in Figures (5) & (6).

The XRD spectrum of each calcination temperature was compared with the XRD spectrum of standard  $\gamma$ -alumina Card JCPDS-files no.29.0063 (Joint Committee on Powder Diffraction Standards) standard mode to assess the purity and phase of synthesized alumina. According to the XRD spectrum of  $\gamma$ -alumina (600-650°C) depicted in Figures (5) & (6).

Fig. (5): XRD of nano  $\gamma$ -alumina powder at  $600\text{ }^{\circ}\text{C}$ Fig. (6): XRD of nano  $\gamma$ -alumina powder  $650\text{ }^{\circ}\text{C}$ 

Three strong peaks are observed and more closely to the standard gamma- alumina as shown in Table (3).

**Table (3) Comparison between standard gamma-alumina and prepared gamma-alumina ( $600, 650^{\circ}\text{C}$ )**

<i>Pos. <math>^{\circ}2\theta</math> 600<math>^{\circ}\text{C}</math></i>	<i>Height [cts]</i>	<i>d-spacing [<math>\text{\AA}</math>]</i>	<i>Pos. <math>^{\circ}2\theta</math> 650<math>^{\circ}\text{C}</math></i>	<i>Height [cts]</i>	<i>d-spacing [<math>\text{\AA}</math>]</i>	<i>Pos. <math>^{\circ}2\theta</math> standard</i>	<i>Heigh [cts]</i>	<i>d-spacing [<math>\text{\AA}</math>]</i>
36.7423	208.41	2.44609	37.4857	120	2.39729	37.6	311	2.39
44.6274	210.34	2.03050	46.0926	233	1.96769	45.96	400	1.98
65.9133	394.00	1.41715	66.3639	555	1.40746	66.761	440	1.40



According to the data shown in Table (3), the produced gamma-alumina at the calcination temperature of 650°C is the most similar to the standard gamma-alumina. When the intensity and d-spacing values are compared, an increase in intensity indicates that a crystal structure contains more atoms in a given plane or that more counts accumulate in this orientation, resulting in a high crystallinity [10].

While calcination temperatures of 500 and 550 °C show that the intensity peaks are not apparent and overlap with one other when compared to the standard scheme (JCPDS) card no. 29.0063 of gamma alumina, Some tendency of phase transformation had begun to develop at these temperatures, with some gamma-alumina peaks at two angles of (49.9433 and 66.0218°) at 500 °C and (66.1936°) at 550° C showing the tendency of becoming obvious as shown in Figures (7) & (8), indicating that the phase of gamma-alumina is not completely amorphous.[11]

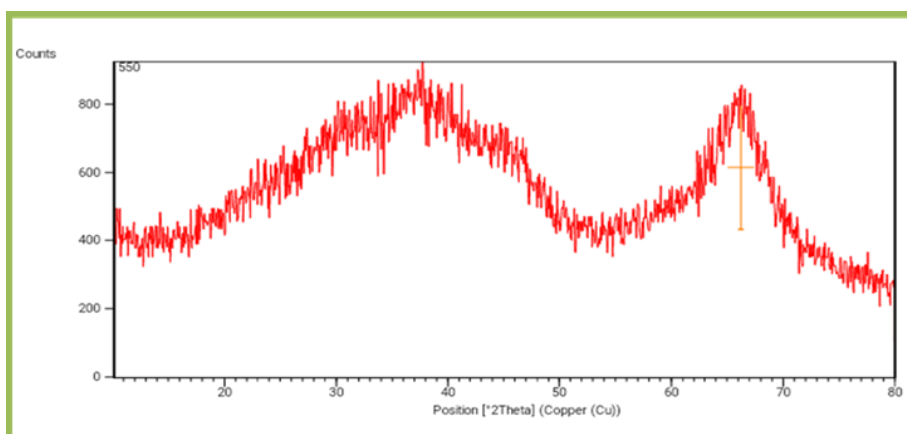


**Fig. (7): XRD of nano  $\gamma$ -alumina powder at 500°C**

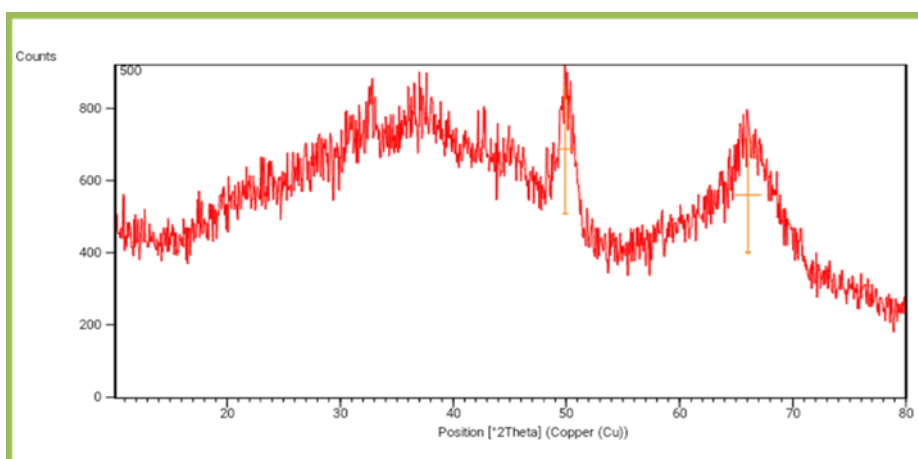


**Fig. (8): XRD of nano  $\gamma$ -alumina powder 550°C**

The % crystallinity of the samples at 600 and 650 °C is calculated by comparing the ratio of the intensity of the peaks for the produced alumina to the corresponding ratios for the standard - alumina samples [11], [12] based on the results in Table (4).

Therefore, Crystallinity % is determined as follows:

$$\text{Crystallinity\%} = \frac{\sum I_{\text{sample}}}{\sum I_{\text{reference}}}$$

As a result, the crystallinity of -alumina at a calcination temperature of 600°C is 84.2 percent and 85.3 percent at a temperature of 650°C.

Furthermore, the three principal reflections of the prepared nano-Al<sub>2</sub>O<sub>3</sub> phase are detected as wide peaks at theta values of (36.7423°, 44.6274°, and 65.9133°) for 600°C and (37.4857°, 46.0926°, and 66.3639°) for 650°C, respectively. Such behavior shows that the larger the width of the peaks, the more crystals are found, but the smaller the size inside the crystalline plane is seen, resulting in the production of nano-sized -Al<sub>2</sub>O<sub>3</sub> crystallites.

Scherrer's equation  $e$  may be used to predict crystallite size as follows [10], [11], [12],[13]:

$$d = 0.94\lambda/\beta \cos \Theta \quad \dots\dots\dots(5)$$

here  $d$ = Diameter of crystallite,  $\lambda$ = X-ray wavelength,  $\beta$  = Broadening line at the half-maximum intensity which represents the full width at half maximum (FWHM),  $\Theta$  = Bragg angle at which the scattering wave was reflected scattered at lattice plane producing intense peaks.

For the obtained nano–alumina powder, the average diameter of the crystallite at 600°C is 26.45 nm and at 650°C is 25.27 nm. It has also been explicitly stated that the ideal calcination temperature to offer the greatest features such as crystallinity, purity, and clarity of the gamma phase is 650°C.

Other parameters, including surface area, thermal stability, and surface acidity, must be evaluated to select the best sample of - alumina with the best attributes. Then, it will be improved with carbon Nanofiber, which will undoubtedly increase the effectiveness of the created catalyst [12].

**Table (4) Comparing the ratio of intensity peaks for the prepared alumina with reference alumina**

<i>Calcination temperature</i>	<i>°2θ Theta</i>	<i>intensity I</i>	<i>Intensity reference. I</i>
600° C	65.9133	100	100
	44.6274	53.4	80
	36.7423	52.9	65
650 °C	66.3639	100	100
	46.0926	59	80
	37.4857	50	65

### 4.3 Surface area and pore volume of $\gamma$ -alumina

The surface area, pore volume, pore size, and density of synthesized nano $\gamma$ -alumina are summarized in Table (5). The data show that raising the calcination temperature from 500 to 600°C causes a rise in surface area and pore volume from (269.44 m<sup>2</sup>/g and 0.674 cm<sup>3</sup>/g) to (327.25 m<sup>2</sup>/g and 0.818 cm<sup>3</sup>/g). At 650°C, there is a reduction in surface area (218.45 m<sup>2</sup>/g) and pore volume (0.546 cm<sup>3</sup>/g). As seen in Table 5, there is a consistent rise in pore size and density from 500 to 600°C, followed by a reduction at 650°C. This increase in the surface area and pore volume as the calcination temperature increases are due to the release of water, including free water, adsorbed water, water in layers, and structure water. Due to an amorphous structure phase that may be created, the removal of Polyethylene glycol used as a linker agent leads to the creation of a considerable number of pores and internal surface area. This can explain why the surface area at 600°C has the highest value.

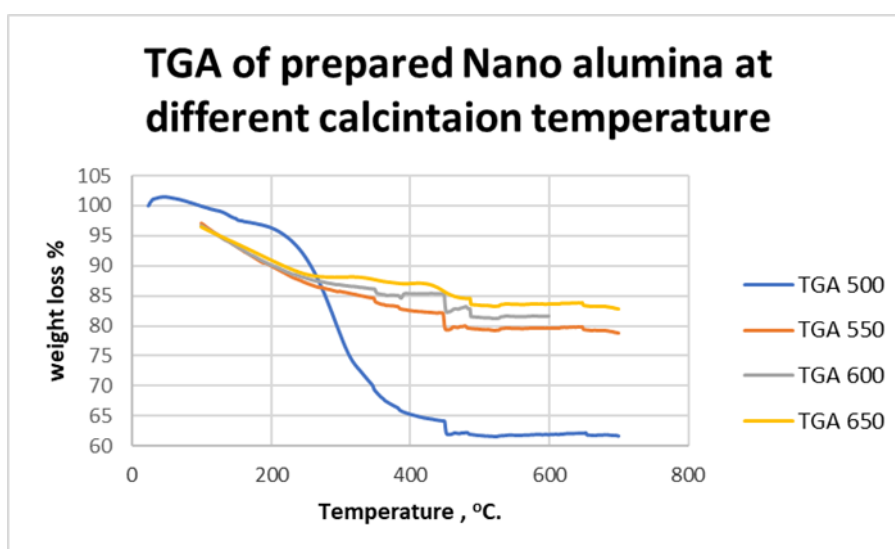
While the decrease in the surface area and pore volume at a calcination temperature of 650°C is due to the phase transformations of a crystalline phase of gamma alumina.[13], [14]

Table (5) The surface area and pore volume of  $\gamma$ -alumina

Calcination temperature °C	Surface area, m <sup>2</sup> /g	Pore volume cm <sup>3</sup> /g	Pore size cm <sup>3</sup>	Bulk density g/cm <sup>3</sup>
500	269.44	0.674	4.8644	0.808
550	315.89	0.789	5.2063	0.945
600	327.25	0.818	5.4177	0.982
650	218.45	0.546	4.8528	0.655

#### 4.4 Thermal gravimetric analysis (TGA) of prepared $\gamma$ -alumina

The TGA profiles of the prepared nano  $\gamma$ -alumina which was calcined at different temperatures (500, 550, 600, and 650°C) are shown in Figures (9) & (10). It can be seen that there is a gradual increase in the percentage of lost weight (21.1959%, 26.5744%, 26.6287%) from a calcination temperature of 500 °C until 600 °C, after that, the loss percentage is dramatically reduced to 12.4506% at a calcination temperature of 650°C, as shown in Figures (9).



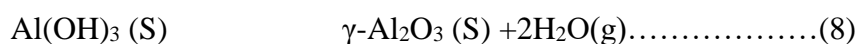
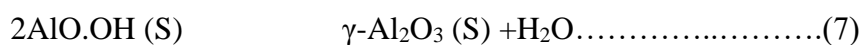
**Fig. (9): Thermogravimetric analysis (TGA) of prepared nano alumina.**

Furthermore, it can be observed that there is a percentage of weight reduction of around 6.5 percent, 8 percent, 10%, and 4.5 percent, respectively. result of the evaporation of physically adsorbed water on the sample surface (dehydration) caused by warming areas from 25°C to 125°C degrees in an air furnace [7].

In the temperature range of 125-250°C, weight loss percentages of roughly 6%, 8.2%, 8%, and 4% were attributed to the loss of chemically combined water (structural water) owing to the synthesis of aluminum oxy-hydroxy, as explained in equation 6 [15], [16].



Also, as stated in equations (7, 8) [16], around 9 percent, 11 percent, 8 percent, and 7 percent of the weight loss percentages, respectively, may be attributed to heating from 250 to 500°C owing to dehydroxylation and calcination stages.



The transition of aluminum hydroxide to alumina was caused by dehydroxylation. TGA curves in Figure (9) indicated a rather stable thermal profile, however it can be seen that the best thermal stability is reached by a sample calcined at 650°C, with a mass loss of roughly 5%. (14.57 percent). This is owing to alumina's phase stability and high purity with excellent crystallization.

#### 4.5 Fourier Transport Infrared (FTIR) of prepared $\gamma$ -alumina

The FTIR spectra of the prepared nano  $\gamma$ -alumina has shown in Figure (10) below.

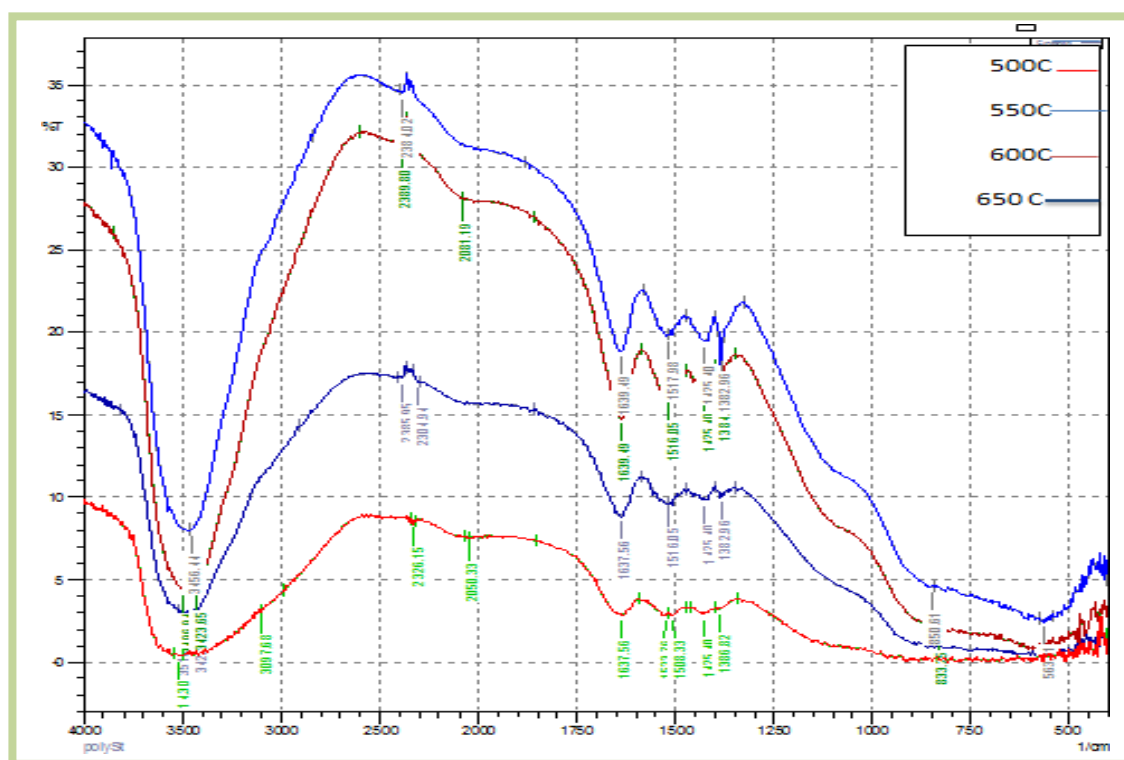


**Fig. (10): FTIR-spectra of the prepared nano  $\gamma$ -alumina at 500, 550, 600, and 650 °C**

It can be seen from wide broadband between 900 and 500  $\text{cm}^{-1}$  due to the Al-O-Al band. The stretching vibration of the Al-O-Al bond and broadening of this band is due to the distribution of vacancies among the octahedral and tetrahedral sites leading to a spreading out of the Al-O vibration frequencies.

There are bands at the surface owing to chemisorbed and adsorbed compounds in addition to alumina bands. The broad bands between 500-750  $\text{cm}^{-1}$  refer to gamma-alumina with nanoparticle size (A large number of atoms in a crystalline nucleus and the existence of amorphous structure or disordered defects [17]).

The superposition of bound hydroxyl groups, isolated OH groups, and stretching vibrations of adsorbed water molecules resulted in the huge band centered at 3000-3850  $\text{cm}^{-1}$ . This indicates the presence of high acidity on the surface of the prepared alumina which improves the attraction between the surface and other organic compounds such as organosulfur compounds. Owing to the molecular water bends, the band 1517.9, 1516.05  $\text{cm}^{-1}$  appears and (C=O) is responsible for the peak at 1637-1639  $\text{cm}^{-1}$ . There are also some strong, complex O-H bending mode bands between 1338-1700  $\text{cm}^{-1}$  that decreased with increasing the calcination temperature. It is also reported that

an H-O-H scissor mode, associated with water species, is found at  $1620\text{cm}^{-1}$  [28]. There are a few different types of functional groups on the surface of the alumina nanoparticles such as hydroxy groups and oxy groups are found [7], [13].

Based on the all-foregoing characterizations such as XRF, XRD, BET, TGA, and FTIR, the samples that are calcined at a temperature of 600 and 650°C are very close in properties such as mechanical strength, thermal stability, crystallinity, high purity, and surface properties or morphology. But the surface area and pore volume of 600°C is considered better than the 650°C as shown in Table (5).

## **5. Conclusion**

A valuable nanoparticle gamma alumina catalyst with high industrial qualification. Despite the increased crystallinity obtained at higher temperatures, investigations revealed that calcination at 600 °C is convenient for producing high crystalline structures due to the energy-saving aspect. Also important is the pH of precipitating aluminum oxide in the neutral region, which can produce a high surface area of crystalline at  $327\text{ m}^2/\text{g}$  and with good thermal stability.

## References

- [1] T. Ivas *et al.*, “Optimization of the calcination temperature for the solvent-deficient synthesis of nanocrystalline gamma-alumina,” *Chem. Pap.*, vol. 73, no. 4, pp. 901–907, 2019. <https://doi.org/10.1007/s11696-018-0637-x>
- [2] S. S. Milani, M. G. Kakroudi, N. P. Vafa, M. M. Mokhayer, and S. H. Gharamaleki, “Properties of alumina sol prepared via inorganic route,” *Ceram. Int.*, vol. 46, no. 7, pp. 9492–9497, 2020. <https://doi.org/10.1016/j.ceramint.2019.12.210>
- [3] N. S. Ahmedzeki, S. J. Hussein, and W. A. Abdulnabi, “Synthesis of Nano Crystalline Gamma Alumina from Waste Cans”, *IJCPE*, vol. 19, no. 1, pp. 45–49, Mar. 2018.
- [4] K. A. M. Jawad, U. A. Saed, and H. H. Alwan, “Synthesis of Nano Platinum-Tungsten Supported on Gamma-Alumina Catalyst,” in *IOP Conference Series: Materials Science and Engineering*, 2020, vol. 928, no. 2, p. 22103. DOI: <https://doi.org/10.1088/1757-899X/928/2/022103>
- [5] N. S. Ahmedzeki, S. Hussein, and W. A. Abdulnabi, “Recycling waste cans to nano gamma alumina: Effect of the calcination temperature and pH,” *Int. J. Curr. Eng. Technol*, vol. 7, no. 1, pp. 82–88, 2017.
- [6] P. Nayar, S. Waghmare, P. Singh, M. Najar, S. Puttevar, and A. Agnihotri, “Comparative study of phase transformation of Al<sub>2</sub>O<sub>3</sub> nanoparticles prepared by chemical precipitation and sol-gel auto combustion methods,” *Mater. Today Proc.*, vol. 26, pp. 122–125, 2020. <https://doi.org/10.1016/j.matpr.2019.05.450>
- [7] A.-H. A. K. Mohammed, H. Q. Hussein, and M. S. Mohammed, “The Effect of Temperature on the Synthesis of Nano-Gamma Alumina Using Hydrothermal Method,” *Iraqi J. Chem. Pet. Eng.*, vol. 18, no. 1, pp. 1–16, 2017.
- [8] Z. Gholizadeh, M. Ghominejad, and F. S. Tehrani, “High Specific Surface Area  $\gamma$ -Al<sub>2</sub>O<sub>3</sub> Nanoparticles Synthesized by Facile and Low-cost Co-precipitation Method,” 2022. <https://doi.org/10.1038/s41598-023-33266-0>
- [9] N. M. Julkapli and H. Md Akil, “X-ray powder diffraction (XRD) studies on kenaf dust-filled chitosan bio-composites,” in *AIP Conference Proceedings*, vol. 989, no. 1, pp. 111–114, 2008. <https://doi.org/10.1063/1.2906040>
- [10] F. B. Afruz and M. J. Tafreshi, “Synthesis of  $\gamma$ -Al<sub>2</sub>O<sub>3</sub> nanoparticles by different combustion modes using ammonium carbonate,” 2014.
- [11] N. K. Renuka, A. V. Shijina, and A. K. Praveen, “Mesoporous  $\gamma$ -alumina nanoparticles:



- synthesis, characterization and dye removal efficiency,” *Mater. Lett.*, vol. 82, pp. 42–44, 2012. <https://doi.org/10.1016/j.matlet.2012.05.043>
- [12] M. Safaei, “Effect of phase-type in the alumina precursor on the flash calcination synthesis,” *Boletín la Soc. Española Cerámica y Vidr.*, vol. 61, no. 5, pp. 552–560, 2022. <https://doi.org/10.1016/j.bsecv.2021.04.004>
- [13] M. Safaei, “Effect of temperature on the synthesis of active alumina by flash calcination of gibbsite,” *J. Aust. Ceram. Soc.*, vol. 53, no. 2, pp. 485–490, 2017. <https://doi.org/10.1007/s41779-017-0058-2>
- [14] A. Amirsalari and S. F. Shayesteh, “Effects of pH and calcination temperature on structural and optical properties of alumina nanoparticles,” *Superlattices Microstruct.*, vol. 82, pp. 507–524, 2015. <https://doi.org/10.1016/j.spmi.2015.01.044>
- [15] Y. M. Chen, M. K. Wang, P. M. Huang, T. M. Tsao, and K. C. Lin, “Influence of catechin on precipitation of aluminum hydroxide,” *Geoderma*, vol. 152, no. 3–4, pp. 296–300, 2009. <https://doi.org/10.1016/j.geoderma.2009.06.017>
- [16] T. P. M. Chu *et al.*, “Synthesis, characterization, and modification of alumina nanoparticles for cationic dye removal,” *Materials (Basel)*, vol. 12, no. 3, p. 450, 2019. <https://doi.org/10.3390/ma12030450>
- [17] S. Dey, “Synthesis and application of  $\gamma$ -alumina nanopowders.” 2014 .